

Gaussian Process Cosmography

Arman Shafieloo¹, Alex G. Kim², Eric V. Linder^{1,2,3}

¹ *Institute for the Early Universe WCU, Ewha Womans University, Seoul, Korea*

² *Lawrence Berkeley National Laboratory, Berkeley, CA 94720, USA and*

³ *University of California, Berkeley, CA 94720, USA*

(Dated: July 11, 2012)

Gaussian processes provide a method for extracting cosmological information from observations without assuming a cosmological model. We carry out cosmography – mapping the time evolution of the cosmic expansion – in a model-independent manner using kinematic variables and a geometric probe of cosmology. Using the state of the art supernova distance data from the Union2.1 compilation, we constrain, without any assumptions about dark energy parametrization or matter density, the Hubble parameter and deceleration parameter as a function of redshift. Extraction of these relations is tested successfully against models with features on various coherence scales, subject to certain statistical cautions.

I. INTRODUCTION

Cosmic acceleration is a fundamental mystery of great interest and importance to understanding cosmology, gravitation, and high energy physics. The cosmic expansion rate is slowed down by gravitationally attractive matter and sped up by some other, unknown contribution to the dynamical equations. While great effort is being put into identifying the source of this extra dark energy contribution, the overall expansion behavior also holds important clues to origin, evolution, and present state of our universe.

Indeed, by studying the expansion as a whole one sidesteps the issue of exactly how to divide the gravitationally attractive (e.g. the imperfectly known matter density) and the accelerating contributions, and whether they are independent or have some interaction (see, e.g., [1–3]). By concentrating on the kinematic variables – the expansion properties as a function of redshift z or scale factor $a = 1/(1+z)$ – one does not need to know the internal structure of the field equations, i.e. the dynamics. The clarity and focus on kinematics trades off against the loss of information on the specific dynamics.

Another gain comes from using geometric measurements – cosmic-distance variables that do not depend on the particular forces and mass densities. The sensitivity of Type Ia supernova measurements of the distance-redshift relation to the deceleration parameter was used to discover the accelerated expansion [4, 5]. Other probes such as gravitational lensing, galaxy-clustering statistics, cluster-mass abundances, etc. provide valuable information, but are dependent on non-kinematic variables. Some techniques, such as distances from baryon acoustic oscillations and Sunyaev-Zel’dovich effects in clusters, are on the fence, nominally geometric but having implicit dependence on the gravitational interaction of matter and so the force law dynamics.

Given distance and redshift measurements, the cosmic expansion rate is related by a derivative of the data, and the deceleration parameter by a further derivative. This is problematic for data with real world noise, as the differentiation further amplifies the noise. Various smooth-

ing procedures have been suggested, e.g. [6], but tend to induce bias in the function reconstruction due to parametric restriction of the behavior or to have poor error control. Using a general orthonormal basis or principal component analysis is another approach, to describe the distance-redshift relation (e.g. [7]) or the deceleration parameter [8], or using a correlated prior for smoothness on the dark energy equation of state [9], but in practice a finite (and small) number of modes is significant beyond the prior, essentially reducing to a parametric approach. Gaussian processes [10] offer an interesting possibility for improving this situation.

Gaussian processes (GP) have been used recently [11–13] in a dynamical reconstruction, going from a set of realizations of the equation of state parameter $w(z)$ of the dark energy component forward to comparison of the derived distance-relation to the distance data. The comparison was carried out through a Markov Chain Monte Carlo (MCMC) assessment of likelihoods. Note that the GP interpolation does not occur between data points but rather on an arbitrary grid of some possibly unmeasured quantity. This approach is intriguing, but relies on separation of the matter density from the dark energy behavior, i.e. it works within a dynamical framework.

The approach in this paper takes a fundamentally different path. We begin with the observations of supernova distances and here consider only kinematic quantities. Modeling the cosmic distance relation as a smooth kinematic function drawn from a GP, the value of the function at any redshift is then predicted directly through testing the GP model against the data. The cosmic expansion can then be extracted from the means and covariance matrices of the Gaussian process realizations (weighted by a posterior) directly for quantities related linearly to the original GP, even through derivatives. This allows us to probe the rate and acceleration of the cosmic expansion in a highly model-independent manner (at the price of focusing on only this type of information). One can view this as a top-down approach, complementary with the bottom-up approach of starting with theoretical quantities and working toward the data, and then applying a likelihood comparison.

In Sec. II we lay out the basics of the kinematic cosmology quantities and the Gaussian process formalism. Readers familiar with the method or eager for results could go to Sec. III where we analyze the results of performing the GP reconstruction, for both current and simulated data. We summarize the cosmological implications and discuss the prospects in Sec. IV. Appendices present details of tests of the robustness of the statistical techniques.

II. COSMOGRAPHIC RECONSTRUCTION

A. Expansion History

Homogeneity and isotropy determine the metric of the universe to be of the Robertson-Walker form, which for a spatially flat universe (from a theory or inflationary prior) is

$$ds^2 = -dt^2 + a^2(t) [dr^2 + r^2(d\theta^2 + \sin^2\theta d\phi^2)] , \quad (1)$$

where t is a time coordinate and r the coordinate distance. The key quantity is the cosmic expansion or scale factor $a(t)$, or equivalently the redshift $z = a^{-1} - 1$.

Without using any field equations, such as the Friedmann equations (the Einstein equations specialized to the above metric) – and hence in a purely kinematic way – we can still define a conformal distance

$$\eta \equiv \int \frac{dt}{a} = \int dr , \quad (2)$$

and build a luminosity distance $d_L(a) = a^{-1}\eta(a)$, and an angular diameter distance $d_a(a) = a\eta$ if desired.

Flux and redshift measurements of a set of standardized candles such as Type Ia supernovae deliver observational access to $\eta(z)$. From this function directly comes the inverse Hubble parameter

$$H^{-1}(z) \equiv \left(\frac{\dot{a}}{a}\right)^{-1} = \frac{d\eta}{dz} \quad (3)$$

and the deceleration parameter

$$q(z) = -\frac{a\ddot{a}}{\dot{a}^2} = -\frac{1+z}{H^{-1}} \frac{dH^{-1}}{dz} - 1 . \quad (4)$$

This a top-down approach, starting with observable distances and proceeding to cosmological kinematic quantities.

We follow this top-down approach because of its useful properties of direct relation to kinematics, avoidance of reliance on a cosmological model or knowledge of the matter density, and well defined and efficient error propagation within the GP method.

An alternative approach with different characteristics is bottom-up. There, one would either parametrize $q(a)$ (or perhaps a dark energy equation of state, or pressure to density, ratio $w_{de}(a) = [2q(a) - 1]/[3\Omega_{de}(a)]$, which

involves the dimensionless dark energy density Ω_{de}) or choose realizations of $q(a)$ from a statistical distribution. Parametrizing $q(a)$ allows straightforward error propagation up to the distances, for comparison to the data; however one must ensure that the parametrization does not restrict or bias the results. Note that choosing a form $q(a)$ is an explicitly dynamical assumption, breaking the kinematic nature of the analysis [14]. In terms of the equation of state, the w_0 - w_a form $w_{de}(a) = w_0 + w_a(1-a)$ is highly robust, reconstructing $d_L(a)$ to better than 0.1% for a wide array of models [15] but does require a separation into matter density and dark energy behavior.

If one uses statistical realizations of $q(z)$, then the error propagation necessary, including the covariances between values i at different redshifts, is

$$\begin{aligned} \text{Cov}[H_i, H_j] &= H_i H_j \times \\ &\int_0^{z_i} \frac{dz'}{1+z'} \int_0^{z_j} \frac{dz''}{1+z''} \text{Cov}[q_i, q_j] \\ \text{Cov}[d_i, d_j] &= (1+z_i)(1+z_j) \times \\ &\int_0^{z_i} \frac{dz'}{H(z')} \int_0^{z_j} \frac{dz''}{H(z'')} \text{Cov}[H_i, H_j] . \end{aligned} \quad (5)$$

This can be slow numerically, especially in a MCMC likelihood evaluation.

However, for a GP the relation between the covariance of a quantity and its derivative (as we use in the top-down approach) is particularly simple and furthermore one can avoid functional parametrizations or statistical distributions of the cosmological variables.

B. Gaussian Process Modeling

We begin with the assumption that the stochastic data is described by a Gaussian process that corresponds to the cosmological function $\eta(z)$. The effective supernova magnitudes at peak brightness, m , and their associated covariance are derived from light-curve data [e.g. 16]. Those peak magnitudes transformed by $(1+z)10^{m/5}$ represent measurements of the conformal distance with a nuisance normalization factor, $y(z) = 10^{M/5} (10\text{pc})^{-1} \eta(z)$ where M is the absolute supernova magnitude.

Derivatives of Gaussian processes are themselves Gaussian processes (with some ignorable pathological exceptions). This means that the estimator for the Hubble length $H^{-1}(a)$ is also a GP (this does not hold for non-flat universes). The deceleration parameter is not a GP because of its nonlinear relation to H^{-1} but its mean value and covariance can be estimated analytically from the two GP functions, dy/dz and d^2y/dz^2 , that it depends on. That is,

$$H^{-1}(a) \propto \frac{dy}{dz} \quad (6)$$

$$q(a) = -(1+z) \left(\frac{dy}{dz}\right)^{-1} \frac{d^2y}{dz^2} - 1 . \quad (7)$$

1. Gaussian Process of the Kinematic Function

The Gaussian processes serve as a regression tool to infer directly from distance data the kinematic expansion properties as a function of redshift z . This provides the covariances between the values at different redshifts as well, which one would expect a physical function to have.

A Gaussian process is defined as a collection of random variables, any finite number of which have a joint Gaussian distribution [10]. A GP $f(z)$ is specified by a mean function $m(z)$ and a covariance function or kernel $k(z, z')$. For a finite set Z of z 's, values of the function are drawn from a Normal distribution, $\mathbf{f} \sim \mathcal{N}(m(Z), K(Z, Z))$ where the matrix element $K_{ij} = k(Z_i, Z_j)$.

The mean function $m(z)$ is an initial guess for the function, in effect ‘‘pre-whitening’’ the data to reduce the dynamic range over which the variations need to be fit. Without sufficient care the results can in fact be influenced by the mean function, so for example assuming a Λ CDM concordance relation is not necessarily a good choice. We discuss the issues in Appendix A where we compare several approaches to choosing a mean function and investigate their influence. In the main text we adopt an iterated smoothings set for the mean function and verify that the final results are not influenced by this input.

For the covariance function we use a common form, the squared exponential [27],

$$k(z, z') = \sigma_f^2 \exp\left(-\frac{|z - z'|^2}{2l^2}\right), \quad (8)$$

where σ_f defines the overall amplitude of the correlation (one can think of this as an offset or tilt of the reconstructed function from the input mean function), and l gives a measure of the coherence length of the correlation. These effects are discussed and illustrated in Appendix B.

Any parameters for the mean function (such as fiducial Ω_m and w , which we do not use), and σ_f^2 and l , are hyperparameters in the fit.

2. Gaussian Process of the Data

In addition to the regression variation represented by the GP covariance function, in the data there is intrinsic dispersion in the distance indicator and (possibly correlated) measurement noise. The sum of all these gives the GP of the measured data \mathbf{y} , with covariance function

$$k_y(z_i, z_j) = k(z_i, z_j) + \sigma_I^2 \delta_{ij} + N(\mu_i, \mu_j), \quad (9)$$

where σ_I^2 is the intrinsic dispersion and $N(\mu_i, \mu_j)$ is the measurement noise covariance matrix.

Note that because $q(z)$ involves a ratio of distance derivatives, it is immune to the absolute amplitude of the distance, i.e. H_0 or its combination with the absolute supernova magnitude \mathcal{M} . In using the smoothing method to generate the mean functions for the GP (see Appendix A) we fit out the absolute amplitude, making the kinematics independent of these nuisance parameters. Fitting for \mathcal{M} is a key step that should not be neglected, and its uncertainties must be propagated into the final reconstruction uncertainties. Fixing it to a particular value can also bias the results. The smoothing method has been shown robust for including \mathcal{M} in [25], and a similar approach has been used in [17] in reconstruction of the expansion history of the universe by combining a smoothing method and Crossing Statistic [18, 19].

3. Inferring Kinematic Functions from Data

Given data \mathbf{y} measured at a set of points Z we want a faithful reconstruction of the distance η , as well as its derivatives, at some other set of points Z_1 . Call the reconstructed function \mathbf{f} . In GP, the joint probability distribution is given by

$$\begin{bmatrix} \mathbf{y} \\ \mathbf{f} \end{bmatrix} \sim \mathcal{N}\left(\begin{bmatrix} \mathbf{m}(Z) \\ \mathbf{m}(Z_1) \end{bmatrix}, \begin{bmatrix} K_y(Z, Z) & K(Z, Z_1) \\ K(Z_1, Z) & K(Z_1, Z_1) \end{bmatrix}\right). \quad (10)$$

Here the subscript y is just to clearly indicate the GP of the input data. The conditional distribution of \mathbf{f} given the data is described by

$$\begin{aligned} \bar{\mathbf{f}} &= m(Z_1) + K(Z_1, Z)K_y^{-1}(Z, Z)\mathbf{y} \\ \text{Cov}(\mathbf{f}) &= K(Z_1, Z_1) - K(Z_1, Z)K_y^{-1}(Z, Z)K(Z, Z_1). \end{aligned} \quad (11)$$

(12)

The probability distribution functions (PDFs) of the reconstructed functions (see Eq. A1 for details) are integrated over the hyperparameter space, weighted by the hyperparameter posterior distribution. For each point in hyperparameter space the PDF of the GP function and its derivatives (e.g. the distance, Hubble length, and second derivative entering the deceleration parameter) can be written analytically:

$$\begin{bmatrix} \mathbf{y} \\ \mathbf{f} \\ \mathbf{f}' \\ \mathbf{f}'' \end{bmatrix} \sim \mathcal{N}\left(\begin{bmatrix} \mathbf{m}(Z) \\ \mathbf{m}(Z_1) \\ \mathbf{m}'(Z_1) \\ \mathbf{m}''(Z_1) \end{bmatrix}, \begin{bmatrix} \Sigma_{00}(Z, Z) & \Sigma_{00}(Z, Z_1) & \Sigma_{01}(Z, Z_1) & \Sigma_{02}(Z, Z_1) \\ \Sigma_{00}(Z_1, Z) & \Sigma_{00}(Z_1, Z_1) & \Sigma_{01}(Z_1, Z_1) & \Sigma_{02}(Z_1, Z_1) \\ \Sigma_{10}(Z_1, Z) & \Sigma_{10}(Z_1, Z_1) & \Sigma_{11}(Z_1, Z_1) & \Sigma_{12}(Z_1, Z_1) \\ \Sigma_{20}(Z_1, Z) & \Sigma_{20}(Z_1, Z_1) & \Sigma_{21}(Z_1, Z_1) & \Sigma_{22}(Z_1, Z_1) \end{bmatrix}\right), \quad (13)$$

where

$$\Sigma_{\alpha\beta} = \frac{d^{(\alpha+\beta)}K}{dz_i^\alpha dz_j^\beta}, \quad (14)$$

and a prime indicates d/dz .

The inferred mean and covariance of the derivatives

are given by

$$\begin{bmatrix} \bar{\mathbf{f}} \\ \bar{\mathbf{f}}' \\ \bar{\mathbf{f}}'' \end{bmatrix} = \begin{bmatrix} \mathbf{m}(\mathbf{Z}_1) \\ \mathbf{m}'(\mathbf{Z}_1) \\ \mathbf{m}''(\mathbf{Z}_1) \end{bmatrix} + \begin{bmatrix} \Sigma_{00}(Z_1, Z) \\ \Sigma_{10}(Z_1, Z) \\ \Sigma_{20}(Z_1, Z) \end{bmatrix} \Sigma_{00}^{-1}(Z, Z) \mathbf{y} \quad (15)$$

$$\text{Cov} \left(\begin{bmatrix} \mathbf{f} \\ \mathbf{f}' \\ \mathbf{f}'' \end{bmatrix} \right) = \begin{bmatrix} \Sigma_{00}(Z_1, Z_1) & \Sigma_{01}(Z_1, Z_1) & \Sigma_{02}(Z_1, Z_1) \\ \Sigma_{10}(Z_1, Z_1) & \Sigma_{11}(Z_1, Z_1) & \Sigma_{12}(Z_1, Z_1) \\ \Sigma_{20}(Z_1, Z_1) & \Sigma_{21}(Z_1, Z_1) & \Sigma_{22}(Z_1, Z_1) \end{bmatrix} - \begin{bmatrix} \Sigma_{00}(Z_1, Z) \\ \Sigma_{10}(Z_1, Z) \\ \Sigma_{20}(Z_1, Z) \end{bmatrix} \Sigma_{00}^{-1}(Z, Z) [\Sigma_{00}(Z, Z_1), \Sigma_{01}(Z, Z_1), \Sigma_{02}(Z, Z_1)]. \quad (16)$$

For $q(z)$, which is not a GP, the mean is given by Eq. (7) and its variance is

$$\text{Var}[q(z)] = (q+1)^2 \left[\frac{\text{Var}[y'(z)]}{y'^2(z)} + \frac{\text{Var}[y''(z)]}{y''^2(z)} - 2 \frac{\text{Cov}[y'(z), y''(z)]}{y'(z)y''(z)} \right]. \quad (17)$$

To integrate over the hyperparameter space (with its non-Gaussian posterior) we can either perform a Monte Carlo integration or do grid sampling. Since we only have two hyperparameters, σ_f^2 and l , we use grid sampling, equispaced in logarithm with priors of $10^{-5} \leq \sigma_f^2 \leq 1$ and $10^{-2} \leq l \leq 10^{0.2} = 1.6$. The final reconstructed results are weighted averages from the posterior based on results from all points in the sampled hyperparameter space. See Appendix B for further details.

C. Data and Simulations

To test the robustness of the reconstruction we perform cosmographic fits to simulated data, and then we also perform fits to actual current data. For current data we use the Union2.1 supernova compilation, including full error covariance matrix, consisting of 580 distances from $z = 0.02 - 1.4$. The simulated data consists of the same number over the same range, realizing distances using a random intrinsic dispersion of 6% in distance, for various input cosmologies.

These different cosmologies are intended both to test the robustness of the GP reconstruction and to explore the discriminatory power of the reconstruction. They are summarized in Table I and all have dimensionless present matter density $\Omega_m = 0.27$. One is a Λ CDM cosmology. Another is a member of the family of mirage models [20], which match the distance to CMB last scattering of Λ CDM, using the relation for the dark energy equation of state $w_a = -3.63(1 + w_0)$. In the limit that $w_0 = -1$ this family reduces to Λ CDM. Note their phantom crossing of $w = -1$ can give unusual features in $q(z)$

that are useful for testing the GP reconstruction. The last model is a rapidly evolving dark energy cosmology with a sharp transition between a high redshift value of the dark energy equation of state parameter $w = -0.5$ and a low redshift value $w = -1$. The specific $w(z)$ is given by the CCL or ‘‘kink’’ form [21] with the same parameters used in [12]. This is a much more rapid transition, and at a lower redshift, than expected in general from dark energy, and so also poses a challenging test of reconstruction.

Cosmology	Description
Λ CDM	$\Omega_m = 0.27, w = -1$
Mirage	$\Omega_m = 0.27, w_0 = -0.7, w_a = -1.09$
Kink	$\Omega_m = 0.27, w_0 = -1, w(z \gg 0.5) = -0.5$

TABLE I: Input cosmologies used to generate simulated distance data from which the GP tries to reconstruct the appropriate kinematic cosmological quantities.

III. EXPANSION HISTORY RESULTS

From many realizations of the GP reconstruction we reconstruct the kinematic functions η , $H^{-1} = \eta'$, and $q(\eta', \eta'')$, where prime denotes d/dz , and their PDFs. We show error bands at every redshift defined such that 68% of the realizations lie within this range. We emphasize that the error band should be interpreted in a redshift by redshift sense and the covariances are not visible in such a plot; that is, the upper part of the band at one redshift may be correlated with the lower part of the band at another redshift.

A. Simulated Data

For each of the cosmologies in Table I we plot $h^{-1} \propto H^{-1}(z)$ in Fig. 1 and $q(z)$ in Fig. 2. The true relations are given for each cosmology by the long, short, and medium dashed curves (the same in all panels of a set). The GP

reconstructions are shown using simulated data based on each cosmology in turn, with 68% error bands. If the error bands fail to overlap the true relation, the GP reconstruction would be inaccurate at 68% confidence level; if the error bands fail to overlap the alternate cosmologies' true relations, GP is successful at distinguishing these models. (Note that these are conservative criteria since even if error band overlaps a true relation this does not necessarily mean agreement with that cosmology because the redshift correlations are not visible.)

We see that each input cosmology is faithfully reconstructed, and each alternate cosmology is properly excluded (at 68% confidence or greater). These results demonstrate that GP can be a useful statistical tool for model independent kinematic parameter estimation.

Agreement of the error band with the input model is a necessary but not wholly sufficient condition for accurate reconstruction. One needs to take into account the correlations between the predictions at each redshift. Rather than do a model by model, full likelihood computation, we tested the influence of correlations between redshifts through model independent, simple statistics. The first used the Om function [22] of the Hubble parameter that serves as a straightforward consistency test of Λ CDM, and the second example used the deceleration parameter. Looking at the distribution of the differences $\Delta Om(0.2, 0.9) \equiv Om(z = 0.2) - Om(z = 0.9)$ and $\Delta q(0.2, 0.9)$, for example, we find agreement with the error band results that the GP reconstructions accurately reproduce the input cosmology values. Since our analysis assumes no dynamics, we do not have to split components into matter and dark energy, and so our results would apply to data generated with different input Ω_m (as we have tested) and even cases with coupling between them.

B. Current Data

We now apply the model-independent constraints from GP to the expansion history reconstructed from actual current data. The Union2.1 compilation [23] carried out a homogeneous, blind, systematics-oriented analysis of supernova distance data. We use their full data covariance matrix for the statistical plus systematics uncertainties. The kinematic reconstruction results are presented in Figs. 3 and 4.

The Λ CDM model with $\Omega_m = 0.27$ (now not an input for the mock data, but a comparison to the fit) is found to be in strong concordance with the Union2.1 data.

However, we cannot distinguish Λ CDM from the mirage family of models, even one with as extreme time variation as $w_0 = -0.7$, $w_a = -1.09$. Partly this is due to the best fit from current data lying between the two, roughly corresponding to a mirage model with $w_0 = -0.85$, $w_a = -0.54$, and partly due to using the full covariance matrix with systematics for current data, which gives larger error bars than the simulated statisti-

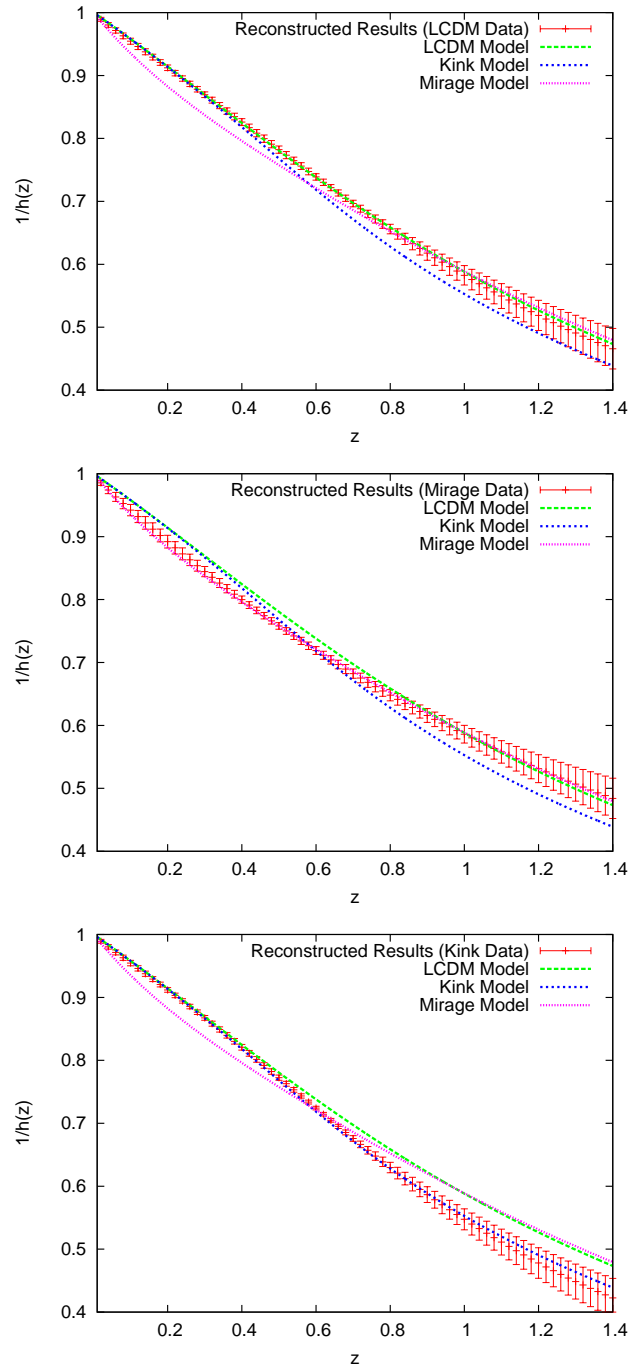


FIG. 1: GP reconstructions of the inverse Hubble parameter $h^{-1}(z) \propto H^{-1}(z)$ are given for simulated data based on the three different input cosmologies of Table I. The dashed curves, the same in all panels, give the true relations. The error band on each reconstruction represents the 68% confidence level. The reconstruction in each case faithfully agrees with the input cosmology.

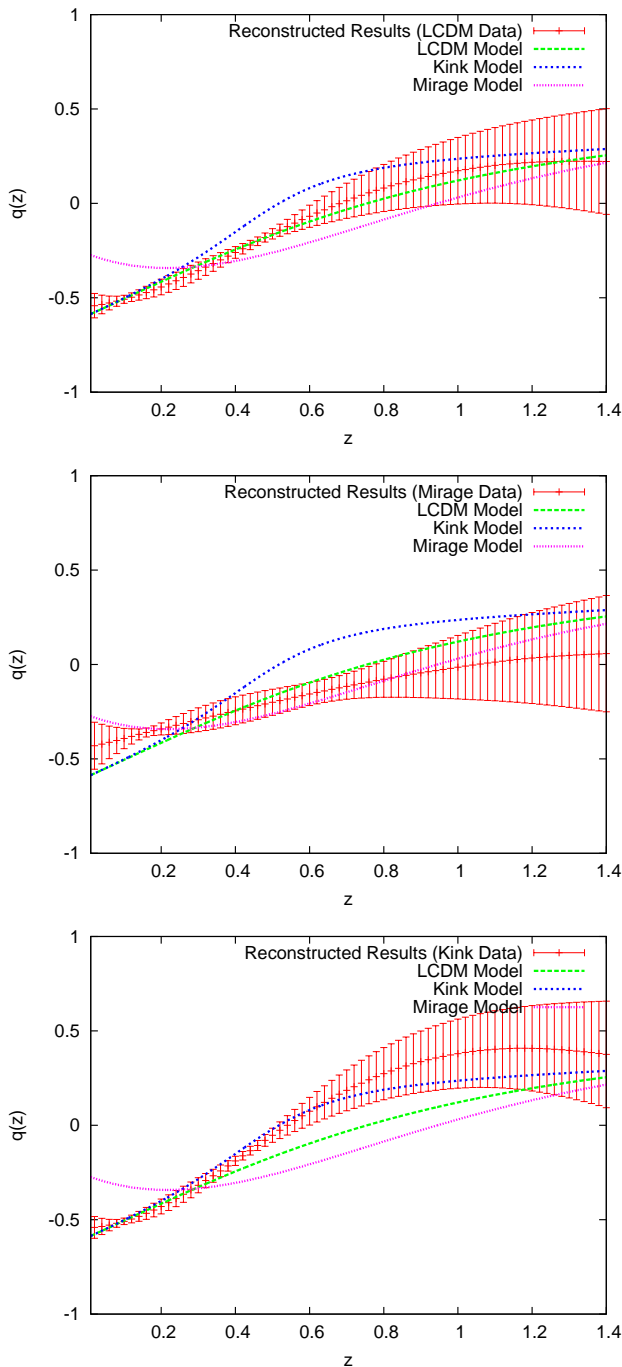


FIG. 2: As Fig. 1, but for the deceleration parameter $q(z)$.

cal errors used in the previous plots.

Current data does point unambiguously to current acceleration in this model independent reconstruction, with $q < 0$ at low redshift with strong significance. However, current kinematic data does not indicate when dark energy fades into the past, i.e. $q > 0$ is not required at $z \gtrsim 1$ from this data.

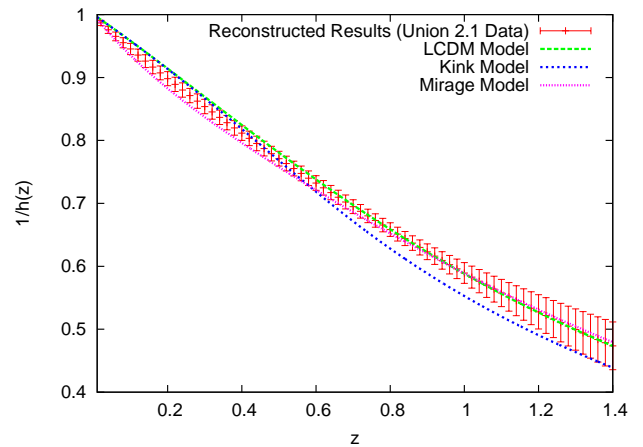


FIG. 3: GP reconstruction of the inverse Hubble parameter $h^{-1}(z) \propto H^{-1}(z)$ using the Union2.1 data compilation is given by the shaded error band representing the 68% confidence level.

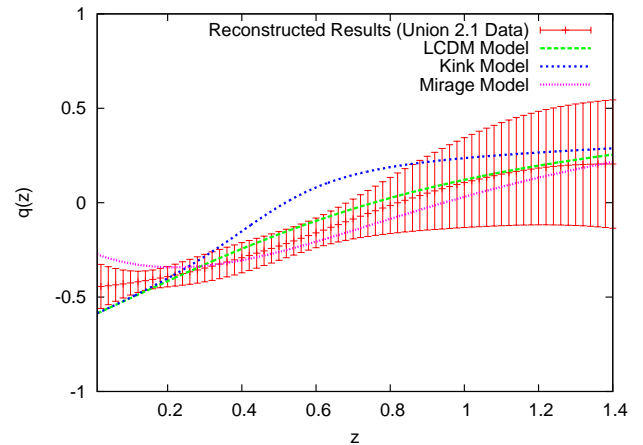


FIG. 4: As Fig. 3, but for the deceleration parameter $q(z)$.

IV. CONCLUSIONS

Gaussian processes can be successfully used in a substantially nonparametric reconstruction of the kinematic quantities characterizing the cosmic expansion. We simulated several cosmologies and found that GP chose the correct one each time. GP also has the advantage of simple, well controlled propagation of errors and covariances to derivatives (or integrals) of the function, allowing distance relations to be converted to the Hubble length or second derivative (which can then be analytically propagated to the deceleration parameter).

Key ingredients entering GP are the mean function and covariance function, with their hyperparameters. We emphasized caution in adopting such functions that might impose (hidden) restrictions on the reconstruction, e.g. through the coherence length, possibly leading to results

retaining memory of the starting point. Proper treatment of hyperparameters through weighted integration over their space and sufficiently wide priors is essential. The combination of smoothing based on the data itself, iteration to remove initial conditions, and a set of mean functions to enable diversity in GP amplitudes and correlations seems to deliver robust results based on our tests. Future work aims at refining this approach further, in particular studying the stability of results for a broad range of input cosmologies.

Our reconstructions of $H^{-1}(z)$ and $q(z)$ using current data are consistent with Λ CDM, but also with cosmologies with substantial time variation. In particular, this holds for the mirage class of models, which preserve the distance to CMB last scattering and so the addition of CMB data to the supernova data will not affect this conclusion. Dynamical probes, such as growth, in combination with the kinematic distance measurements used can have further leverage, but mirage models also have substantially similar growth to Λ CDM; for example our extreme mirage model agrees in growth as a function of redshift to within 1.5% with Λ CDM with the same matter density.

While mirage models cross $w = -1$, no conclusions can be drawn from the data regarding the necessity for such crossing to occur. Furthermore, until future data accuracy constrains the time variation of the equation of state to below $w_a \lesssim 0.5$ (the current best fit mirage value), crossing cannot be said to be tested significantly.

Current distance data has insufficient leverage on the higher order kinematic quantities, such as the deceleration parameter $q(z)$. It does definitely show, by this substantially nonparametric approach, that cosmic acceleration is occurring at low redshift. The transition from acceleration to deceleration, however, could have happened at any redshift $z \gtrsim 0.7$, or even not at all, according to this current data. Future kinematic data extending to redshifts $z \gtrsim 1$ are necessary to resolve all the issues of substantial time variation, phantom crossing, and the onset of acceleration. Future applications of GP include projection of such constraints from future surveys, possibly allowing for spatial curvature, and tests of modified gravity, say, through growth vs. expansion.

Acknowledgments

We thank Rollin Thomas for helpful discussions. This work has been supported by World Class University grant R32-2009-000-10130-0 through the National Research Foundation, Ministry of Education, Science and Technology of Korea and the Director, Office of Science, Office of High Energy Physics, of the U.S. Department of Energy under Contract No. DE-AC02-05CH11231.

Appendix A: GP Mean Function

The GP formalism gives a clear formulation for derivation of the kinematic functions and their derivatives using the data, however there are some practical technical details that require care. One of the important issues is the initial guess for the mean function. The final results turn out not to be independent of this for an arbitrary choice, but can in fact retain some memory of the initial choice, biasing the results.

One reason for this is because of the multiscale nature of the data for an arbitrary cosmology. With two square-exponential-kernel hyperparameters, one for coherence length and one for the amplitude of deviations from the mean function, there exists limited freedom for the GP to track the deviations of the data from the input mean function redshift by redshift. One solution is to use more hyperparameters for the GP covariance function but this leads to a greater computational burden and the possibility of fitting the noise in the data rather than the cosmological signal.

The residuals of the data around different mean functions can be quite different. Certainly there is little expectation that any of these residuals are perfectly described by a Gaussian Process with a particular kernel. It is therefore not unexpected for model predictions from different mean functions to be statistically inconsistent.

To give another view on this, consider the GP likelihood probability in more detail. It contains three parts: the usual χ^2 , the determinant of the GP likelihood function penalizing overcomplexity, and a constant contribution involving the number of data points [10],

$$2 \ln p(y|f) = -y^T \Sigma_{00}(Z, Z)^{-1} y - \ln \det \Sigma_{00}(Z, Z) - n \ln(2\pi), \quad (\text{A1})$$

GP tries to find the best combination of first and second parts to get the highest likelihood. That is, it tries to make f as close as possible to the data y by making minimum changes to the given mean function to get a reasonable χ^2 and at the same time tries to keep the results smooth enough to get a high likelihood from the second term. Note the second term is independent of the data and arises solely from the hyperparameters. (This simplified explanation is somewhat complicated by the weighted integration over the hyperparameter space, but the basic flavor of it holds.)

The ultimate model-independent input mean function is the zero mean function. Here, however, we need a large σ_f to bring f close to y ; to apply this ‘‘correction’’ to zero input over a large redshift range, without merely being a constant offset, requires a large coherence length l . While one might then succeed in fitting f to y , this comes at the price of smoothing away the features and losing accurate reconstruction of y' and y'' . Conversely, if we choose an input mean function that gives f close to y at several redshifts, then GP wants to keep σ_f small to change the input function as little as possible. A small σ_f effectively makes GP moot and so the reconstruction

never strays far from the input function, with the results retaining memory of the input.

We have verified these properties by investigating a large variety of mean functions: 1) zero mean function, 2) flat Λ CDM model with a fixed Ω_m , 3) flat Λ CDM model with Ω_m as an added hyperparameter, 4) flat w CDM model with Ω_m and w as added hyperparameters. The issues raised above show up clearly.

To get around these problems we want to use an input mean function with little cosmology dependence (for robust results), sensitivity to multiple scales (for flexibility in fitting y well enough that the derivatives are reconstructed well), and few added hyperparameters (for computational tractability). The solution we have adopted after extensive testing is an iterated smoothing approach, building on the method developed in [24–26].

We emphasize that the smoothing is only to generate an initial mean function. The data is smoothed over a scale Δ in $\ln(1+z)$, after “pre-whitening” using an initial guess d_L^g [26]:

$$\ln d_L(z, \Delta)^s - \ln d_L(z)^g = N(z) \times \quad (\text{A2})$$

$$\sum_i \frac{\ln d_L(z_i) - \ln d_L(z_i)^g}{\sigma_{d_L(z_i)}^2} \exp \left[-\frac{\ln^2 \left(\frac{1+z_i}{1+z} \right)}{2\Delta^2} \right],$$

$$N(z)^{-1} = \sum_i \exp \left[-\frac{\ln^2 \left(\frac{1+z_i}{1+z} \right)}{2\Delta^2} \right] \frac{1}{\sigma_{d_L(z_i)}^2}. \quad (\text{A3})$$

This procedure is then iterated, with the output of one iteration serving as the initial guess of the successive iteration. The final reconstructed results have been shown to be independent of the first initial guess [24–26]. Because the final iteration is a smooth function, we can take the derivatives of the mean functions as required for computing f' and f'' . To incorporate many scales we actually use a set of 5 initial guess mean functions, iterating each one independently. The scatter in the final mean functions or the appropriate derivatives then is added, weighted by likelihood, as an additional uncertainty, in the statistical sense of the mean squared error known as risk: the quadratic sum of the mean dispersion and the dispersion in the mean. We find that stopping the iteration procedure when the χ^2 of each lies within $\Delta\chi^2 = 2.3$ of each other (equivalent to 1σ for 2 degrees of freedom, hence as much dispersion as from l and σ_f^2) gives robust results, as seen from the accurate reconstructions achieved for the Λ CDM, mirage, and kink simulations. In order to capture the true data it is important to have inputs that can cross the true cosmology over different redshift ranges, so the 5 initial guesses cover a wide range of behaviors, Λ CDM cosmologies with $(\Omega_m, \Omega_\Lambda) = (1, 0), (0, 1), (0, 0), (0.3, 0.7), (0.5, 0.5)$. Note that no additional hyperparameters are introduced.

This iterated smoothing set approach to the mean function has the desired properties of not relying on a specific cosmological form and having freedom from memory of the initial guess, while allowing the GP formalism to balance the different terms in the likelihood and give accurate reconstructions with well characterized errors. The tests run for reconstruction of the different cosmologies as shown in Figs. 1 and 2 demonstrate its success.

Appendix B: Hyperparameter Distribution

The hyperparameters of the covariance function are another ingredient for the GP reconstruction. Each set of hyperparameters, in our case σ_f^2 and l , gives rise to a particular likelihood by Eq. (A1), for each of the five mean functions.

The posterior distribution is derived using Bayes’ theorem

$$P(i, \sigma_f^2, l) = \frac{L(i, \sigma_f^2, l)p(i)p(\sigma_f^2)p(l)}{\sum_{i=1}^5 \int L(i, \sigma_f^2, l)p(i)p(\sigma_f^2)p(l)d \ln \sigma_f^2 d \ln l}, \quad (\text{B1})$$

where i is the index for the five mean functions, $p(i) = 1/5$, and the other priors are flat in the logarithm for $10^{-5} \leq \sigma_f^2 \leq 1$ and $10^{-2} \leq l \leq 1.6$. The lower limit on σ_f^2 and upper limit of l do impose non-trivial truncation of the likelihood surface as discussed below. Note that setting a minimum $l = 10^{-2}$ is equivalent to imposing a blurring on the square-exponential kernel, and prevents fitting to merely noise in the data. Realizations of f , f' , and f'' are drawn from the Gaussian Process models represented by this posterior.

Figure 5 illustrates the role of σ_f^2 and l in the reconstruction. Basically σ_f acts to set the amplitude for deviations from the mean function and l controls the wiggliness, or coherence scale.

As discussed in Appendix A, a small value of σ_f^2 represents little contribution of GP to the reconstruction process, i.e. the result is basically just the mean function. Large values of l smooth over features in the data and basically give merely an offset that could be absorbed in the amplitude. If we included arbitrarily small σ_f^2 or large l in the hyperparameter ranges, these regions of the space would give nearly identical likelihoods and dilute the overall probabilities, biasing the results toward the mean function. To avoid this situation we impose the lower limit $\log \sigma_f^2 \geq -5$ (i.e. ignoring models changing the mean function by less than 0.7%) and the upper limit $l \leq 1.6$ (i.e. the range of the data). We have checked that the final best fits for the hyperparameters are not significantly affected by small variations in the priors.

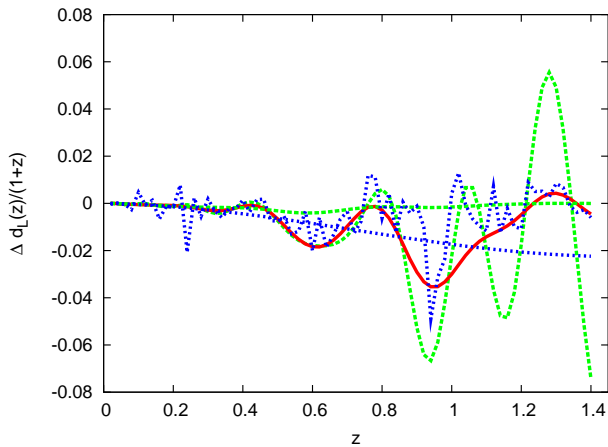


FIG. 5: Schematic plot of the effects of σ_f and l on the reconstruction function $f(z)$. The solid red curve has $l = 0.1$ and $\sigma_f^2 = 0.001$ and will serve as a reference. The two dark blue dotted lines show the impact of changing l , with $l = 0.01$ (wiggly line) and $l = 1.0$ (nearly smooth line), keeping σ_f unchanged. The two light green dashed lines show the impact of changing σ_f , with $\sigma_f^2 = 0.1$ (increased amplitude of deviations in $f(z)$) and $\sigma_f^2 = 0.00001$ (decreased amplitude), keeping l at the reference value. For very small values of σ_f^2 , GP makes very little contribution (near zero modification at all scales), while for high values of l possible features of the data might be smoothed out.

-
- [1] M. Kunz, Phys. Rev. D 80, 123001 (2009) [arXiv:astro-ph/0702615]
- [2] M. Kunz, A.R. Liddle, D. Parkinson, C. Gao, Phys. Rev. D 80, 083533 [arXiv:0908.3197]
- [3] A. Aviles & J.L. Cervantes-Cota, Phys. Rev. D 84, 083515 [arXiv:1108.2457]
- [4] S. Perlmutter *et al.*, Astrophys. J. **517**, 565 (1999) [arXiv:astro-ph/9812133]
- [5] A. G. Riess *et al.*, Astron. J. **116**, 1009 (1998) [arXiv:astro-ph/9805201]
- [6] V. Sahni and A. A. Starobinsky, Int. J. Mod. Phys. D **15**, 2105 (2006) [arXiv:astro-ph/0610026]
- [7] S. Benitez-Herrera, F. Roepke, W. Hillebrandt, C. Mignone, M. Bartelmann, J. Weller, MNRAS 419, 513 (2012) [arXiv:1109.0873]
- [8] C. Shapiro & M.S. Turner, ApJ 649, 563 (2006) [arXiv:astro-ph/0512586]
- [9] R.G. Crittenden, G-B. Zhao, L. Pogosian, L. Samushia, X. Zhang, JCAP 1202, 048 (2012) [arXiv:1112.1693]
- [10] C. E. Rasmussen & C. K. I. Williams, Gaussian Processes for Machine Learning, MIT Press (2006) www.GaussianProcess.org/gpml
- [11] T. Holsclaw, U. Alam, B. Sanso, H. Lee, K. Heitman, S. Habib, D. Higdon, Phys. Rev. D 82, 103502 (2010) [arXiv:1009.5443]
- [12] T. Holsclaw, U. Alam, B. Sanso, H. Lee, K. Heitman, S. Habib, D. Higdon, Phys. Rev. Lett. 105, 241302 (2010) [arXiv:1011.3079]
- [13] T. Holsclaw, U. Alam, B. Sanso, H. Lee, K. Heitman, S. Habib, D. Higdon, Phys. Rev. D 84, 083501 (2011) [arXiv:1104.2041]
- [14] E.V. Linder, Rept. Prog. Phys. 71, 056901 (2008) [arXiv:0801.2968]
- [15] R. de Putter, E.V. Linder, JCAP 0810, 042 (2008) [arXiv:0808.0189]
- [16] J. Guy, P. Astier, S. Baumont et al, A&A, 466, 11 (2007) [arXiv:astro-ph/0701828]
- [17] A. Shafieloo, arXiv:1204.1109
- [18] A. Shafieloo, T. Clifton and P. Ferreira, JCAP 1108, 017 (2011) [arXiv:1006.2141]
- [19] A. Shafieloo, JCAP 1205, 024 (2012) [arXiv:1202.4808]
- [20] E.V. Linder, arXiv:0708.0024
- [21] P.S. Corasaniti, E.J. Copeland, Phys. Rev. D 67, 063521 (2003) [arXiv:astro-ph/0205544]
- [22] V. Sahni, A. Shafieloo and A. A. Starobinsky, Phys. Rev. D **78**, 103502 (2008) [arXiv:0807.3548]
- [23] N. Suzuki et al., ApJ 746, 85 (2012) [arXiv:1105.3470]
- [24] A. Shafieloo, U. Alam, V. Sahni and A. A. Starobinsky, Mon. Not. Roy. Astron. Soc. **366**, 1081 (2006) [arXiv:astro-ph/0505329]
- [25] A. Shafieloo, Mon. Not. Roy. Astron. Soc. **380**, 1573 (2007) [arXiv:astro-ph/0703034]
- [26] A. Shafieloo and C. Clarkson, Phys. Rev. D **81**, 083537 (2010) [arXiv:0911.4858]
- [27] K must be positive definite for any set of z 's. The squared exponential form is at the limit of this condition so we

actually use an exponent of 1.999 rather than 2, as did [\[11\]](#).